Research articles

Creating skyrmions and skyrmioniums using oscillating perpendicular magnetic fields

H. Vigo-Cotrina[a,*], A.P. Guimarães[a]

[a] Centro Brasileiro de Pesquisas Físicas, 22290-180 Rio de Janeiro, RJ, Brazil

ABSTRACT

Magnetic skyrmions and skyrmioniums are exotic magnetic configurations that have several potential applications in Spintronics. In this work, using micromagnetic simulations, we show that it is possible to create metastable skyrmions and skyrmioniums in an isolated cobalt nanodisk, that has as its minimum energy configuration a single domain with perpendicular magnetization. First, we have determined the ground state of the nanodisk and the frequencies of the spin wave modes of skyrmions and skyrmioniums for different values of perpendicular uniaxial anisotropy constant K_z and Dzyaloshinskii-Moriya exchange constant D_{int}. Next, in order to create a skyrmion or skyrmionium, we have applied an oscillating perpendicular magnetic field with a frequency equal to that of the spin wave modes. Our results show that it is possible to switch from single domain to skyrmion or skyrmionium, tuning parameters such as the intensity of the applied perpendicular magnetic field, and its duration.

1. Introduction

Non-trivial topologically protected spin textures, such as magnetic skyrmions, can be created in ferromagnetic nanostructures with different geometries [1–7]. Magnetic skyrmions are characterized by the topological charge Q. For skyrmions with polarity p = + 1, i.e., magnetization at the center in the +z direction, the topological charge is Q = 1, and for skyrmions with polarity p = −1, the topological charge is Q = −1 [6,8].

The topological protection of magnetic skyrmions allows them to evade obstacles or defects in the nanostructures as they move [9], and also coexist in the form of clusters, without mutual annihilation [10]. Magnetic skyrmions can be moved with small current densities [8], reducing the undesirable Joule heating that is detrimental in Spintronics applications, e.g., racetrack memories [11].

Skyrmioniums, also called target skyrmions [12] or 2π-skyrmions [13], are another type of spin texture similar to skyrmions, that can also be created in ferromagnetic nanostructures [14–16,12,17,18]. A skyrmionium can be considered as a combination of two skyrmions with opposite topological charge [17,12], resulting in a total topological charge Q = 0. This allows the skyrmionium, unlike the skyrmion, to move without suffering deflections due to the skyrmion Hall effect (SkHE). This property is essential to read and write information in potential applications of skyrmioniums as components of devices for

magnetic recording [18].

Skyrmioniums can reach higher velocities in comparison with a skyrmion [19,17], another property that is relevant for applications in Spintronics.

Skyrmioniums in magnetic nanostructures arise in micromagnetic simulations [20,15,21] and have been experimentally observed at low temperature and room temperature [12,22–24]. They can be created in ferromagnetic nanostructures by tuning parameters such as the ratio of the thickness to the radius of the nanodisk, perpendicular magnetic anisotropy, and Dzyaloshinskii-Moriya interaction [20], or using an external perturbation, e.g., spin polarized current [15], and static perpendicular magnetic field [25,14,12].

However, it is necessary to look for methods that allow us to have selectivity in creating either magnetic skyrmions, or skyrmioniums, in an isolated nanostructure.

In the present work, we propose a simple method to create selectively these textures, in a nanodisk with a perpendicularly magnetized single-domain, using oscillating perpendicular magnetic fields with frequencies equal to the frequencies of the spin wave modes of these textures. To demonstrate this idea, we used the open source code Mumax3 [26], with a cell size $1 \times 1 \times L$ nm^3, where L is the thickness of the nanodisk. We assumed T = 0 K, however, the present method is valid at room temperature (see Supplementary material). The material used was Cobalt with parameters [20,27]: saturation magnetization

$M_s = 5.8 \times 10^5$ A/m, exchange stiffness $A_{ex} = 15$ pJ/m, perpendicular uniaxial anisotropy constant $K_z = 0.8$ and 1.0 MJ/m^3, and Dzyaloshinskii-Moriya exchange constant D_{int} ranging between 3.4 and 4.0 mJ/m^2.

2. Results and discussion

We have simulated a thin Cobalt nanodisk deposited on a Pt substrate (Co/Pt), with diameter D = 150 nm and thickness L = 1 nm.

First, in order to obtain the relaxed magnetic state of the nanodisk, we have considered in our micromagnetic simulations three initial magnetic configurations: perpendicular single domain, skyrmion, and skyrmionium. The energies of the relaxed states are shown in Fig. 1. These were obtained using a large damping constant of $\alpha = 0.3$ for faster convergence. For all our values of D_{int} and K_z, it was possible to obtain three final magnetic states, except for $D_{int} = 3.8$ mJ/m^2, where it was possible to obtain only two final magnetic states. The state of lowest energy in all cases, as shown in Fig. 1, is a magnetic single domain.

In order to obtain the spin wave modes, a skyrmion or skyrmionium configuration was chosen as the initial magnetic state in the nanodisk, and then relaxed[1]. Afterwards, we have applied a perpendicular sinc magnetic pulse field $B_z = B_0 \text{Sinc}(2\pi f(t-t_0))$, centered on $t_0 = 1$ ns, where $B_0 = 5$ mT is the magnetic field amplitude, and f = 70 GHz is the cutoff frequency[2]. The spatial profile of the z-component of the magnetization was saved every 5 ps for a total simulation time of 20 ns. In this process we have used a lower damping constant $\alpha = 0.002$, for better resolution of the spin wave modes. The same procedure was repeated for a skyrmionium configuration as initial magnetic state.

The power spectrum was calculated by a fast Fourier transform (FFT) of the z-component of the magnetization, using all cells of the nanodisk (see Ref. [29] for details) from the temporal evolution of the spatial profile of the z-component of the magnetization obtained in the previous step. In Fig. 2 are shown the power spectra of a skyrmion (Fig. 2(a)), and of a skyrmionium (Fig. 2(b)), for the parameters $K_z = 0.8$ MJ/m^3 and $D_{int} = 3.4$ mJ/m^2. The power spectra shown in Fig. 2 have prominent peaks[3], indicating the frequencies of the spin wave modes. For the skyrmion, there are three peaks at approximately 7.79 GHz (mode 1), 59.59 GHz (mode 2), and 68.23 GHz (mode 3); for a skyrmionium, three prominent peaks at approximately 3.69 GHz (mode 1), 24.04 GHz (mode 2), and 60.73 GHz (mode 3).

The spatial distribution of FFT power of the spin wave modes is shown in Fig. 2(c) and (d). For the skyrmion, mode 1 (breathing mode) corresponds to maximum oscillation amplitudes distributed near the center of nanodisk (see color bar in Fig. 2), whereas mode 2 and mode 3 correspond to maximum oscillation amplitudes distributed both in the center and on the edges. For the skyrmionium, mode 1 and mode 2 correspond to maximum oscillation amplitudes distributed in the center of the nanodisk, and mode 3 is more intense at the edges of the nanodisk Fig. 2(d).

In order to excite the spin wave modes and create skyrmions and skyrmioniums, we have used an oscillating perpendicular magnetic field $B_z = B_0 \sin(2\pi f t)$, where B_0 is the magnetic field intensity and f is the frequency of the spin wave modes obtained from the curve of spectral density, and shown in Fig. 2(a) and (b).

It is important to note here that continuum transitions between magnetic configurations with different values of topological charge are possible in nanosystems [30,31], because in these systems the
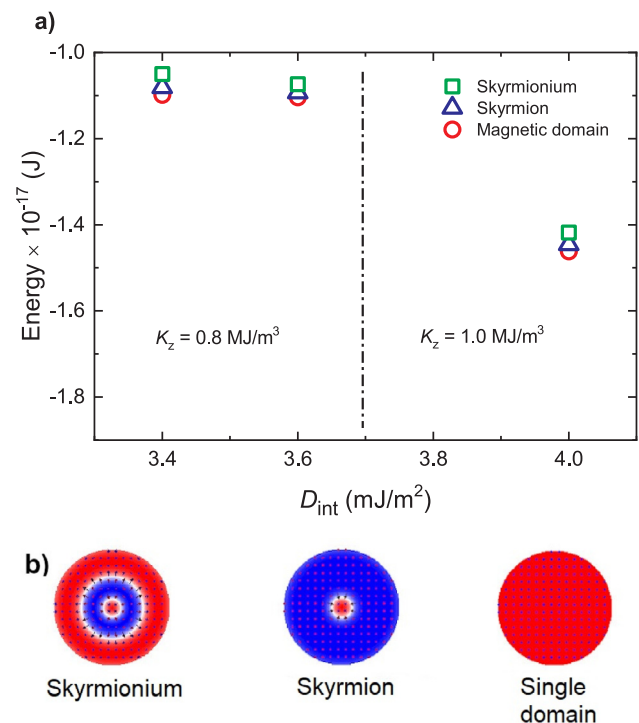

Fig. 1. (a) Energy of the final magnetic states of the nanodisk vs. Dzyaloshinskii-Moriya exchange constant D_{int}, and (b) in-plane view of the z-component of the magnetization for a skyrmionium, skyrmion, and magnetic single domain.

continuity is broken by the edges or through the applications of magnetic fields or spin currents, allowing transitions between magnetic configurations with different values of the topological charge [30,31], as shown by several works [15,16,18,31–34].

In order to create a skyrmion in the nanodisk, we started with a nanodisk in the single domain state, with perpendicular magnetization (t = 0 ns). Next, we have applied the oscillating magnetic field[4]. The temporal evolution of the z-component of the magnetization is shown in Fig. 3(a–c) for all spin wave modes. In this figure, we can see that the dynamics of this component, before the skyrmion is created, is different for each mode. This difference is related to the spatial distribution of the spin wave modes in the nanodisk (see Fig. 2(c)).

From magnetic single domain to skyrmion: We encountered that a skyrmion can be created for all values of the frequencies of the peaks corresponding to the spin wave modes shown in Fig. 2(a), and that the threshold of magnetic field intensity and the duration of the applied field necessary to create the skyrmion depend on the frequency of the spin wave mode. For example, for the first mode, we have obtained a skyrmion applying a magnetic field of $B_0 = 926$ mT during t = 900 ps. Once the magnetic field is turned off, the system is allowed to relax until the skyrmion is created (Fig. 3(a)). The created skyrmion shrinks and expands until it is stabilized at approximately 7.5 ns.

For the second mode, the magnetic field intensity threshold needed to create a skyrmion is $B_0 = 449$ mT, and time of duration t = 640 ps, and for the third mode $B_0 = 888$ mT and t = 510 ps. Note that for mode 1, the skyrmion is created after 1 ns, and for modes 2 and 3, the skyrmion is created before 1 ns, which shows that it is more efficient to use the frequencies of the higher order modes.

---

[1] We have shown only the results for $K_z = 0.8$ MJ/m^3 and $D_{int} = 3.4$ mJ/m^2.

[2] We have used this pulse because it allows exciting all spin wave frequencies present in the system up to a value of f = 70 GHz [14,28].

[3] In some cases there are tiny peaks in the spectrum that can be considered noise or spin wave modes of smaller amplitude. However, we have worked only with the more intense peaks.

[4] For practical reasons, we have considered the application of the oscillating fields for a maximum period of 1 ns. If in this period there was no formation of a skyrmion or a skyrmionium, we increased the value of the magnetic field intensity.
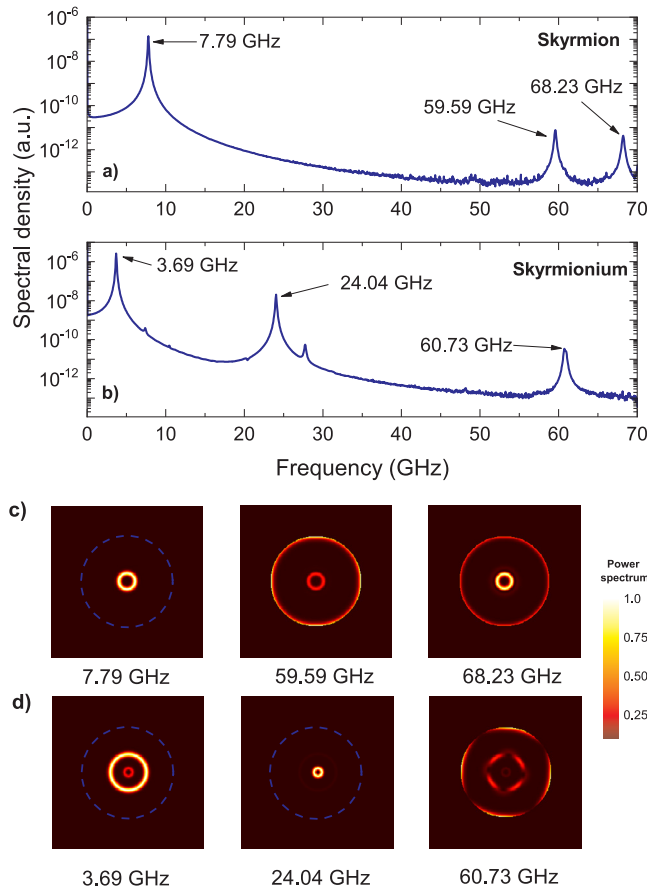
Fig. 2. Power spectrum (a) for a skyrmion and (b) for a skyrmionium, obtained by fast Fourier transform for $K_z = 0.8$ MJ/m^3, and $D_{int} = 3.4$ mJ/m^2. Spatial distribution of the Fourier power of the spin wave modes (c) for a skyrmion and (d) for a skyrmionium. The blue dashed lines in Figure (c) and Figure (d) represent the edges of the nanodisk.
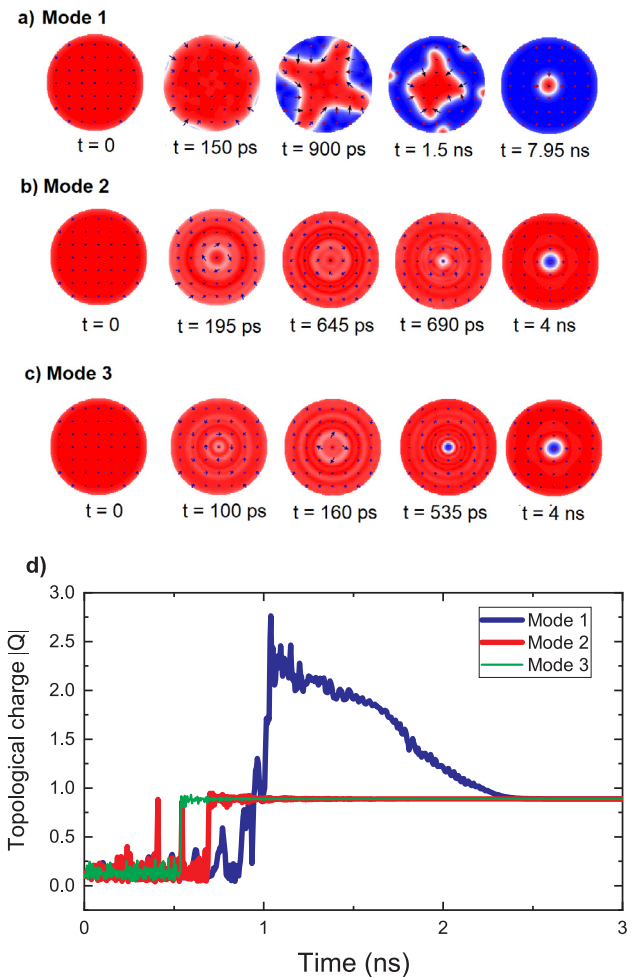
Fig. 3. Images of the nanodisk exhibiting the temporal evolution of the z-component of the magnetization for (a) mode 1, (b) mode 2, (c) mode 3 and (d) temporal evolution of the absolute value of the topological charge for the three modes. Note the superposition of the curves corresponding to modes 2 and 3 for times longer than about 0.7 ns.

The temporal evolution of the absolute value of the topological charge Q is shown in Fig. 3(d). In this figure it is possible to observe that the value of the topological charge Q is approximately 1 before 1 ns for mode 2 and mode 3, and after 1 ns for mode 1.

For mode 1, the topological charge Q increases from approximately $Q \approx 0$ to $Q \approx 2.7$. This increase corresponds to the strange magnetic configurations that appear during and after the application of the oscillating magnetic field (Fig. 3(a)). For mode 2 and mode 3, the evolution of the topological charge is smoother in comparison with mode 1. This is because, unlike the time evolution observed with mode 1, there are no strange magnetic configurations during and after the application of the oscillating magnetic field (Fig. 3(b, c)).

From magnetic single domain to skyrmionium: In order to create a skyrmionium in the nanodisk, we followed the same methodology used for the formation of a skyrmion, again starting from a single domain with perpendicular magnetization. Next, the oscillating perpendicular magnetic field was applied. In this process, it was possible to create a skyrmionium for all values of the frequencies of the spin wave modes shown in Fig. 2(b).

In a way similar to that of the creation of a skyrmion, the temporal evolution of the z-component of the magnetization is different for each spin wave mode, as it is shown in Fig. 4(a–c).

For mode 1, it is possible to obtain a skyrmionium using a value of $B_0 = 998$ mT and duration of applied magnetic field t = 300 ps. After turning off the magnetic field, the system evolves forming several deformed skyrmions, as shown in Fig. 4(a) for t = 345 ps. These later give

rise to a deformed skyrmionium; the created skyrmionium is stabilized in approximately 4 ns.

For mode 2 (Fig. 4(b)), a skyrmionium is created using a value of $B_0 = 969$ mT and duration of applied magnetic field t = 350 ps. Note that the process of creation of skyrmionium is similar to that shown in Fig. 4(a) for mode 1. There appear tiny deformed skyrmions in the nanodisk, which later merge, giving rise to a deformed skyrmionium. The similarity in the dynamics of the z-component of the magnetization, before the skyrmionium is created, arises because mode 1 and mode 2 are similar, both concentrated near the center of the nanodisk (Fig. 2(d)).

For mode 3, a skyrmionium is created using a value of $B_0 = 904$ mT and duration of applied magnetic field t = 430 ps. The process of creation of the skyrmionium is shown in Fig. 4(c). This process is different from the processes for modes 1 and 2. In this case, there appears a skyrmion, with polarity p = +1 (Fig. 4(c) for t = 290 ps), in the center of nanodisk, that shrinks and expands its diameter until finally there appears another core in the center (Fig. 4(c) for t = 445 ps), with polarity p = −1.

The temporal evolution of the absolute value of the topological charge Q is shown in Fig. 4(d). In every case the final value of Q is approximately zero, which confirms the formation of a skyrmionium. In this figure, it is possible to observe that for mode 1, the topological charge initially increases from $Q \approx 0$ to $Q \approx 4$, which suggests the
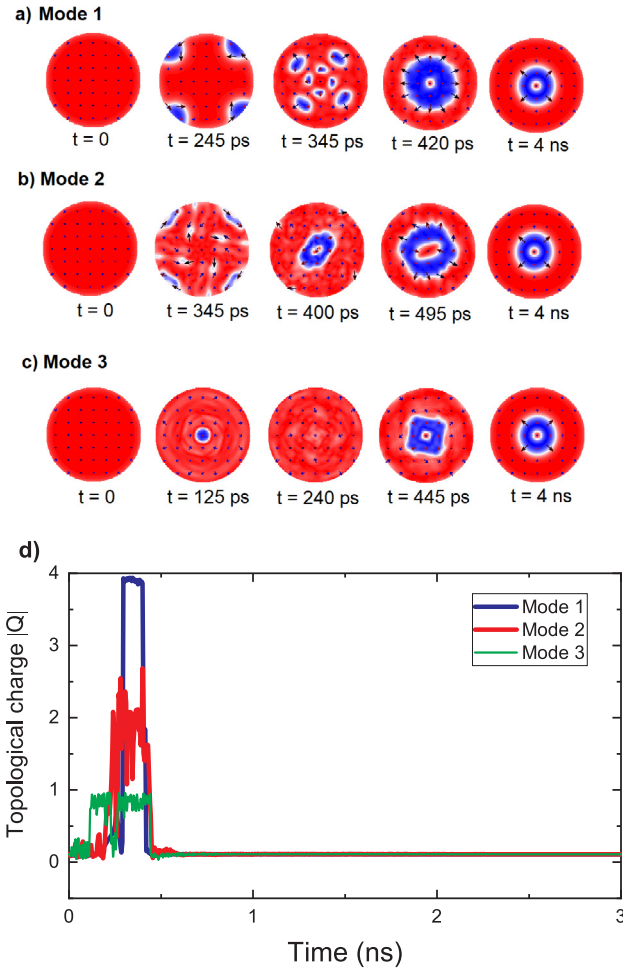
a) Mode 1

b) Mode 2

c) Mode 3

d)

Fig. 4. Images of the nanodisk, exhibiting the temporal evolution of the z-component of the magnetization for (a) mode 1, (b) mode 2, and (c) mode 3 and (d) temporal evolution of the absolute value of the topological charge for the three modes. Note the superposition of the curves corresponding to modes 1, 2 and 3 for times longer than about 0.4 ns.

formation of more than one skyrmion in the nanodisk during the process of creation of the skyrmionium, and that matches the images shown in Fig. 4(a). Afterwards, the value of the topological charge Q goes to approximately zero, which corresponds to the creation of the skyrmionium.

For mode 2, the absolute value of the topological charge Q increases from $Q \approx 0$ to just over $Q = 2$, which also suggests the formation of more than one skyrmion in the nanodisk during the process of formation of the skyrmionium. Next, the value of the topological charge goes to zero.

For mode 3, the absolute value of the topological charge Q increases initially from $Q \approx 0$ to $Q \approx 1$. This suggests the formation of one skyrmion, and matches the images shown in Fig. 4(c). Next, the topological charge goes to approximately zero, confirming the creation of a skyrmionium in the nanodisk.

We have realized simulations (not shown here) for all values of K_z and D_{int} shown in Fig. 1. In all cases it was possible to obtain skyrmions and skyrmioniums. For example, for $K_z = 0.8 \, MJ/m^3$, and $D_{int} = 3.6 \, mJ/m^2$, we have obtained a skyrmion using a value of $B_0 = 927 \, mT$ and duration of applied magnetic field $t = 660 \, ps$ for mode 1 (f = 3.79 GHz), $B_0 = 551 \, mT$, and duration of applied magnetic field $t = 140 \, ps$ for mode 2 (f = 54.19,GHz), and $B_0 = 411 \, mT$ and duration of applied magnetic field $t = 735 \, ps$ for mode 3 (f = 59.94 GHz).

A skyrmionium was obtained using a value of $B_0 = 926 \, mT$ and duration of applied magnetic field $t = 630 \, ps$ for mode 1 (f = 3.65 GHz), $B_0 = 804 \, mT$ and duration of applied magnetic field $t = 510 \, ps$ for mode 2 (f = 14.15 GHz), and $B_0 = 832 \, mT$ and duration of applied magnetic field $t = 285 \, ps$ for mode 3 (f = 62.58 GHz). For $K_z = 1.0 \, MJ/m^3$ and $D_{int} = 4 \, mJ/m^2$, the values of the magnetic field intensity needed to obtain skyrmions and skyrmioniums increase to values above 1 T.

Additionally, in the Supplementary material, we have considered effects of temperature (T = 300 K) in our simulations. Our results show that the principle of selectivy in the creation of a skyrmion or a skyrmionium is still valid. However, an increase in the required values of applied magnetic field and its duration was encountered. This is due to the fact that the temperature can modify the spatial profile of the spin wave modes.

Switching between skyrmion and skyrmionium: Additionally, we also show that it is possible to switch from a magnetic skyrmion configuration to skyrmionium, and vice versa. In this case, we started with a magnetic skyrmion (or skyrmionium) configuration in the nanodisk. Next, as in the previous cases, we applied the oscillating perpendicular magnetic field.

The temporal evolution of the z-component of the magnetization for mode 1 is shown in Fig. 5 for mode 1. For mode 1, we have obtained a skyrmionium from a skyrmion, using a value of $B_0 = 245 \, mT$ and duration of applied magnetic field $t = 216 \, ps$. For this mode, a skyrmion was obtained from a skyrmionium, using a value of $B_0 = 29 \, mT$ and duration of applied magnetic field $t = 80 \, ps$.

The process of switching between skyrmion and skyrmionium was successfully achieved for all values of K_z and D_{int} shown in Fig. 1.

Finally, the skyrmions and skyrmioniums can be deleted, for example, using a static perpendicular magnetic field that saturates the magnetization of the nanodisk, in the z direction.
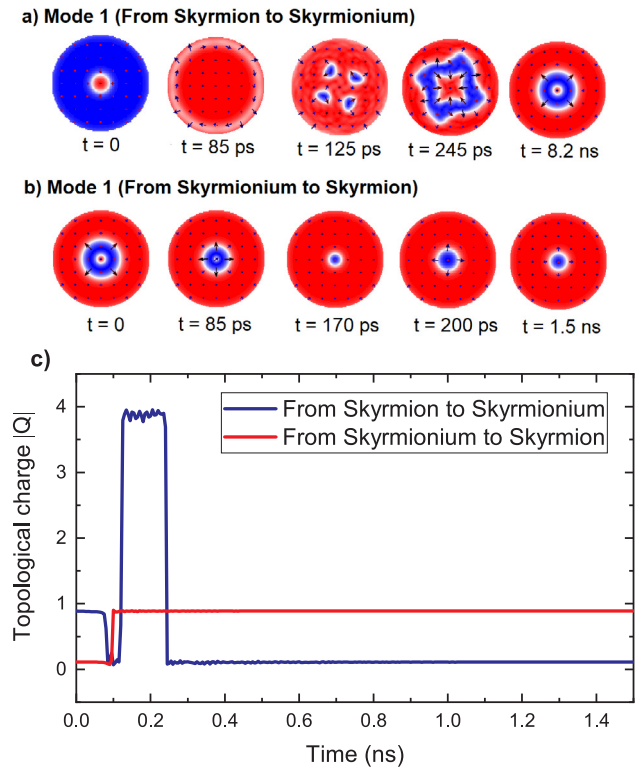
a) Mode 1 (From Skyrmion to Skyrmionium)

b) Mode 1 (From Skyrmionium to Skyrmion)

c)

Fig. 5. Temporal evolution of the configuration of the nanodisk. Images of the nanodisk for (a) from skyrmion to skyrmionium and (b) from skyrmionium to skyrmion; (c) temporal evolution of the absolute value of the topological charge for mode 1.

3. Conclusions

In summary, in this work, we have studied the formation of a skyrmion and a skyrmionium in a Co/Pt nanodisk using micromagnetic simulations. Our results show that a perpendicular oscillating magnetic field can be used to create a skyrmion or a skyrmionium, when the frequency of the magnetic fields is equal to the frequencies of the spin wave modes, and the duration of the pulse is in the sub nanosecond time range.

We have also shown that the process of formation of skyrmions and skyrmioniums is related to the way the spin wave modes are distributed on the nanodisk. Our results also show that the magnetic field intensity and the duration of the applied fields can be tailored in order to create either skyrmions or skyrmioniums. These results are relevant, since this method allows the selective creation of skyrmions or skyrmioniums, depending on the envisaged application, without having to keep the external magnetic field on. In potential applications in magnetic storage devices, this method could be used to switch between a magnetic single domain, that would represent, e.g., the bit 1, and a skyrmion or skyrmionium, that would represent the bit 0.

CRediT authorship contribution statement

H. Vigo-Cotrina: Conceptualization, Methodology, Software, Writing - original draft. **A.P. Guimarães:** Supervision, Writing - review & editing, Resources.

Declaration of Competing Interest

The authors declare that they have no known competing financial interests or personal relationships that could have appeared to influence the work reported in this paper.

Acknowledgments

Appendix A. Supplementary data

Supplementary data associated with this article can be found, in the online version, at https://doi.org/10.1016/j.jmmm.2020.166848.

References

[1] Y. Liu, H. Du, M. Jia, A. Du, Switching of a target skyrmion by a spin-polarized current, Phys. Rev. B 91 (2015) 094425, https://doi.org/10.1103/PhysRevB.91.094425.

[2] X. Zhao, C. Jin, C. Wang, H. Du, J. Zang, M. Tian, R. Che, Y. Zhang, Direct imaging of magnetic field-driven transitions of skyrmion cluster states in FeGe nanodisks, Proc. Natl. Acad. Sci. 113 (18) (2016) 4918–4923, https://doi.org/10.1073/pnas.1600197113.

[3] L. Wang, C. Liu, N. Mehmood, G. Han, Y. Wang, X. Xu, C. Feng, Z. Hou, Y. Peng, X. Gao, G. Yu, Construction of a room-temperature pt/co/ta multilayer film with ultrahigh-density skyrmions for memory application, ACS Appl. Mater. Interfaces 11 (12) (2019) 12098–12104, https://doi.org/10.1021/acsami.9b00155.

[4] S. Saha, M. Zelent, S. Finizio, M. Mruczkiewicz, S. Tacchi, A.K. Suszka, S. Wintz, N.S. Bingham, J. Raabe, M. Krawczyk, L.J. Heyderman, Formation of Néel-type skyrmions in an antidot lattice with perpendicular magnetic anisotropy, Phys. Rev. B 100 (2019) 144435, https://doi.org/10.1103/PhysRevB.100.144435.

[5] X. Liang, G. Zhao, L. Shen, J. Xia, L. Zhao, X. Zhang, Y. Zhou, Dynamics of an antiferromagnetic skyrmion in a racetrack with a defect, Phys. Rev. B 100 (2019) 144439, https://doi.org/10.1103/PhysRevB.100.144439.

[6] A.P. Guimarães, Principles of Nanomagnetism, second ed., Springer, Cham, 2017.

[7] H. Vigo-Cotrina, A. Guimarães, Influence of the dipolar interaction in the creation of skyrmions in coupled nanodisks, J. Magn. Magn. Mater. 489 (2019) 165406, https://doi.org/10.1016/j.jmmm.2019.165406.

[8] X. Zhang, Y. Zhou, M. Ezawa, High-topological-number magnetic skyrmions and topologically protected dissipative structure, Phys. Rev. B 93 (2016) 024415, https://doi.org/10.1103/PhysRevB.93.024415.

[9] A. Fert, V. Cros, J. Sampaio, Skyrmions on the track, Nat. Nanotechnol. 8 (2013) 152, https://doi.org/10.1038/nnano.2013.29.

[10] Y. Liu, H. Yan, M. Jia, H. Du, A. Du, J. Zang, Field-driven oscillation and rotation of a multiskyrmion cluster in a nanodisk, Phys. Rev. B 95 (2017) 134442, https://doi.org/10.1103/PhysRevB.95.134442.

[11] R. Tomasello, E. Martinez, R. Zivieri, L. Torres, M. Carpentieri, G. Finocchio, A strategy for the design of skyrmion racetrack memories, Scientific Rep. 4 (2014) 6784, https://doi.org/10.1038/srep06784.

[12] F. Zheng, H. Li, S. Wang, D. Song, C. Jin, W. Wei, A. Kovács, J. Zang, M. Tian, Y. Zhang, H. Du, R.E. Dunin-Borkowski, Direct imaging of a zero-field target skyrmion and its polarity switch in a chiral magnetic nanodisk, Phys. Rev. Lett. 119 (2017) 197205, https://doi.org/10.1103/PhysRevLett.119.197205.

[13] J. Hagemeister, A. Siemens, L. Rózsa, E.Y. Vedmedenko, R. Wiesendanger, Controlled creation and stability of kπ skyrmions on a discrete lattice, Phys. Rev. B 97 (2018) 174436, https://doi.org/10.1103/PhysRevB.97.174436.

[14] A.C. Booth, Y. Liu, J. Zang, Collective modes of three-dimensional magnetic structures: a study of target skyrmions, J. Magn. Magn. Mater. 489 (2019) 165447, https://doi.org/10.1016/j.jmmm.2019.165447.

[15] X. Zhang, J. Xia, Y. Zhou, D. Wang, X. Liu, W. Zhao, M. Ezawa, Control and manipulation of a magnetic skyrmionium in nanostructures, Phys. Rev. B 94 (2016) 094420, https://doi.org/10.1103/PhysRevB.94.094420.

[16] S.K. Panigrahy, C. Singh, A.K. Nayak, Current-induced nucleation, manipulation, and reversible switching of antiskyrmioniums, Appl. Phys. Lett. 115 (18) (2019) 182403, https://doi.org/10.1063/1.5125290.

[17] S. Li, J. Xia, X. Zhang, M. Ezawa, W. Kang, X. Liu, Y. Zhou, W. Zhao, Dynamics of a magnetic skyrmionium driven by spin waves, Appl. Phys. Lett. 112 (14) (2018) 142404, https://doi.org/10.1063/1.5026632.

[18] B. Göbel, A.F. Schäffer, J. Berakdar, I. Mertig, S.S.P. Parkin, Electrical writing, deleting, reading, and moving of magnetic skyrmioniums in a racetrack device, Scientific Rep. 9 (2019) 12119, https://doi.org/10.1038/s41598-019-48617-z.

[19] A.G. Kolesnikov, M.E. Stebliy, A.S. Samardak, A.V. Ognev, Skyrmionium – high velocity without the skyrmion Hall effect, Scientific Rep. 8 (2018) 16966, https://doi.org/10.1038/s41598-018-34934-2.

[20] X. Liu, Q. Zhu, S. Zhang, Q. Liu, J. Wang, Static property and current-driven precession of 2π-vortex in nanodisk with Dzyaloshinskii-Moriya interaction, AIP Adv. 5 (8) (2015) 087137, https://doi.org/10.1063/1.4928727.

[21] N. Mehmood, X. Song, G. Tian, Z. Hou, Z. Fan, M. Qin, X. Gao, J.-M. Liu, Strain-mediated electric manipulation of magnetic skyrmion and other topological states in geometric confined nanodiscs, J. Phys. D: Appl. Phys. 53 (1) (2019) 014007, https://doi.org/10.1088/1361-6463/ab47bd.

[22] Z. Hou, W. Ren, B. Ding, G. Xu, Y. Wang, B. Yang, Q. Zhang, Y. Zhang, E. Liu, F. Xu, W. Wang, G. Wu, X. Zhang, B. Shen, Z. Zhang, Observation of various and spontaneous magnetic skyrmionic bubbles at room temperature in a frustrated kagome magnet with uniaxial magnetic anisotropy, Adv. Mater. 29 (29) (2017) 1701144, https://doi.org/10.1002/adma.201701144.

[23] D. Cortés-Ortuño, N. Romming, M. Beg, K. von Bergmann, A. Kubetzka, O. Hovorka, H. Fangohr, R. Wiesendanger, Nanoscale magnetic skyrmions and target states in confined geometries, Phys. Rev. B 99 (2019) 214408, https://doi.org/10.1103/PhysRevB.99.214408.

[24] S. Zhang, F. Kronast, G. van der Laan, T. Hesjedal, Real-space observation of skyrmionium in a ferromagnet-magnetic topological insulator heterostructure, Nano Lett. 18 (2) (2018) 1057–1063, https://doi.org/10.1021/acs.nanolett.7b04537 pMID: 29363315..

[25] C. Song, Y. Ma, C. Jin, J. Wang, H. Xia, J. Wang, Q. Liu, Field-tuned spin excitation spectrum of kπ skyrmion, New J. Phys. 21 (8) (2019) 083006, https://doi.org/10.1088/1367-2630/ab348e.

[26] A. Vansteenkiste, J. Leliaert, M. Dvornik, M. Helsen, F. Garcia-Sanchez, B. Van Waeyenberge, The design and verification of Mumax3, AIP Adv. 4 (10) (2014) 107133, https://doi.org/10.1063/1.4899186.

[27] J. Sampaio, V. Cros, S. Rohart, A. Thiaville, A. Fert, Nucleation, stability and current-induced motion of isolated magnetic skyrmions in nanostructures, Nat. Nanotechnol. 8 (2013) 839–844, https://doi.org/10.1038/nnano.2013.210.

[28] J.-V. Kim, F. Garcia-Sanchez, J.a. Sampaio, C. Moreau-Luchaire, V. Cros, A. Fert, Breathing modes of confined skyrmions in ultrathin magnetic dots, Phys. Rev. B 90 (2014) 064410, https://doi.org/10.1103/PhysRevB.90.064410.

[29] A. Baker, M. Beg, G. Ashton, M. Albert, D. Chernyshenko, W. Wang, S. Zhang, M.-A. Bisotti, M. Franchin, C.L. Hu, R. Stamps, T. Hesjedal, H. Fangohr, Proposal of a micromagnetic standard problem for ferromagnetic resonance simulations, J. Magn. Magn. Mater. 421 (2017) 428–439, https://doi.org/10.1016/j.jmmm.2016.08.009.

[30] J. Iwasaki, M. Mochizuki, N. Nagaosa, Current-induced skyrmion dynamics in constricted geometries, Nat. Nanotechnol. 8 (2013) 742–747, https://doi.org/10.1038/nnano.2013.176.

[31] Y. Zhou, M. Ezawa, A reversible conversion between a skyrmion and a domain-wall pair in a junction geometry, Nat. Commun. 5 (2014) 2041–1723.https://doi.org/10.1038/ncomms5652.

[32] H.Y. Yuan, X.R. Wang, Skyrmion creation and manipulation by nano-second current pulses, Scientific Rep. 6 (2016) 22638, https://doi.org/10.1038/srep22638.

[33] J. Wang, C. Jin, C. Song, H. Xia, J. Wang, Q. Liu, Rapid creation and reversal of skyrmion in spin-valve nanopillars, J. Magn. Magn. Mater. 474 (2019) 472–476, https://doi.org/10.1016/j.jmmm.2018.11.036.

[34] G. Yin, Y. Li, L. Kong, R.K. Lake, C.L. Chien, J. Zang, Topological charge analysis of ultrafast single skyrmion creation, Phys. Rev. B 93 (2016) 174403, https://doi.org/10.1103/PhysRevB.93.174403.